Energy-Spectral Efficiency Tradeoff for Heterogeneous Networks with QoS Constraints

Cemil Can Coskun and Ender Ayanoglu
Center for Pervasive Communications and Computing
Department of Electrical Engineering and Computer Science
University of California, Irvine
Irvine, CA 92697-2625

***Abstract*—In this paper, we investigate the energy efficiency (EE) and spectral efficiency (SE) tradeoff in multi-cell heterogeneous networks (HetNets). Our objective is to maximize both EE and SE of the network while satisfying the rate requirement of users. We use multi-objective optimization techniques to define the objective function. We propose a three-stage algorithm in this paper. First, we select the cell-center radius for the fractional frequency reuse (FFR) method. Second, we assign the frequency resources to satisfy the rate requirements of users and maximize the objective function. Third, the power allocation subproblem is solved by using the Levenberg-Marquardt method. Our numerical results show that a Pareto-optimal solution exists for EE and SE. We present results for different rate constraints.**

***Index Terms*—Energy efficiency, spectral efficiency, heterogeneous cellular networks, power control, multi-objective optimization, OFDM.**

I. Introduction

In recent years, the rapid increase of mobile users brought the need for higher throughput and the problem of coverage simultaneously. Increasing the spectral efficiency (SE) of the network can help meet the increasing throughput demand. However, the SE metric does not provide any intuition about the energy efficiency (EE) of the network. In fact, solutions that improve SE may be inefficient in terms of EE. Therefore, an EE metric has been defined in the literature. EE has been investigated in the literature under the topic of "Green Communications," see, e.g, [1] and the references therein.

Heterogeneous networks (HetNets) are investigated in the literature to meet the increasing throughput demand and eliminate coverage holes [2]. Due to the fact that coverage regions of base stations overlap, interference is a significant problem in HetNets. To overcome this problem, intercell interference cancellation and mitigation techniques are investigated in the literature [3], [4]. In this paper, we employ the fractional frequency reuse (FFR) scheme for multi-tier networks that is studied in [5], [6]. FFR is preferred over other solutions for intercell interference due to its low complexity. In [5], same cell-center radius is used in every sector. In our prior work [6], the same FFR scheme is employed, but the cell-center radii were selected depending on the user distribution. In this paper, we employ the same FFR scheme, however we update cell-center boundaries dynamically depending on the network conditions. This approach helps us satisfy the rate requirements of users and improve our objective. Although the FFR scheme mitigates some portion of the interference in the network, intercell interference is still a significant problem. To further suppress the interference, interference-based pricing mechanisms have been studied in the literature, see, e.g., [7]–[9]. In this paper, a similar method has been employed and downlink transmissions of the base stations are penalized with respect to the amount of interference they create. This approach prevents the base stations from increasing their transmission power to levels that decrease the total utility of the network.

As stated earlier, maximizing EE and SE problems usually contradict with each other [10]. Therefore, this tradeoff has attracted significant attention in the literature. In [10], the authors investigate the EE-SE tradeoff in single-cell single-tier networks. They show the EE function is strictly quasi-concave over the SE function. In [11], the EE-SE tradeoff has been investigated in interference-limited networks. The problem is non-convex and NP-hard to solve. Therefore, they propose an iterative power allocation algorithm which guarantees convergence to a local optimum. In [12], the EE-SE tradeoff is investigated for OFDMA networks with optimal joint resource allocation of transmission power and bandwidth. The authors show that when the cell size decreases, the EE of the network increases.

The aforementioned papers investigate maximizing EE and SE problems separately. Another approach to investigate this problem is to combine these metrics under one metric. For this purpose, multi-objective optimization techniques have been widely investigated in the literature [13]. These techniques are successfully used to investigate the EE-SE tradeoff. In [14], [15], the weighted summation method is used to combine the EE and SE metrics. The authors in [14] investigate the EE with proportional fairness for downlink distributed antenna systems. The tradeoff between transmission power and bandwidth requirement in single-tier single-cell networks is investigated in [15]. Authors of this work show that the EE-SE tradeoff can be exploited by balancing the occupied bandwidth and power consumption. In this paper, we investigate the EE-SE tradeoff in multi-cell multi-tier networks. The weighted summation model is implemented to combine EE and SE functions.

The contributions of this paper are as follows. We study the joint maximization of EE and SE in multi-cell heteroge-

This work was partially supported by the National Science Foundation under Grant No. 1307551.

978-1-4673-8999-0/17/$31.00 ©2017 IEEE

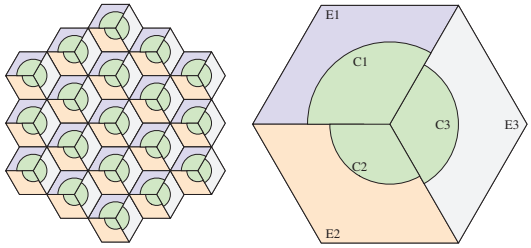

Figure 1. Dynamic cell-center region boundaries in a multi-tier FFR scheme. The network layout assumes a uniform 19-cell hexagonal grid in which the MBSs have three sector antennas and Pico-BSs employ omnidirectional antennas.

Table I
SPECTRUM ASSIGNMENT IN A MULTI-TIER FFR SCHEME

Base Station Type	Sector 1		Sector 2		Sector 3	
	Cell-Center	Cell-Edge	Cell-Center	Cell-Edge	Cell-Center	Cell-Edge
MBS	A	B	A	C	A	D
Pico-BS	C and D	A, C, and D	B and D	A, B, and D	B and C	A, B, and C

neous wireless networks. The rate requirements of users are addressed. We propose a novel three-stage algorithm whereby at each stage the solution is improved. We show that the sacrifices in terms of SE can be transformed into gain in terms of EE or vice versa. We investigate the relation between the EE-SE tradeoff and rate constraints of the users.

The remainder of this paper is organized as follows. Section II introduces the system model, base station power consumption, and the SE and EE definitions. Section III formulates the resource allocation problem. The proposed algorithm is presented in Section IV. Simulation results are discussed in Section V. Section VI concludes the paper.

II. System Model

This section presents our system model, describe the power consumption model of the base stations, and define the SE and EE metrics.

In Fig. 1, a 19-cell hexagonal wireless network is depicted. In this paper, we employ the multi-tier FFR scheme described in [5], [6]. Three-sector antennas are employed in macro base stations (MBS), and omnidirectional antennas are used in picocell base stations (Pico-BSs). The network area is divided into 57 sectors. Each sector area is divided into cell-center and cell-edge regions. The spectrum allocation is shown in Table I. The total bandwidth of the network is divided into 4 disjoint subbands. The number of subcarriers in subbands A, B, C, and D are denoted by N_A, N_B, N_C, and N_D, respectively. The total number of subcarriers is denoted by N, i.e., $N = N_A + N_B + N_C + N_D$.

In this paper, the constant power allocation across the subbands is studied. Two power control parameters are introduced to characterize the power assignment of the base stations: β and ε. The parameter β scales the transmission power of the base stations. The ratio of the transmission power of MBSs on cell-edge to cell-center subcarriers is defined by ε. We can write the signal-to-interference-plus-noise ratio (SINR) of macrocell associated user (MUE) k on subcarrier n as follows

$$\gamma_k^{(n)} = \frac{P_M^{(n)} g_{k,M}^{(n)}}{\sum\limits_{\substack{M' \in \mathcal{B}_M \\ M' \neq M}} P_{M'}^{(n)} g_{k,M'}^{(n)} + \sum\limits_{P \in \mathcal{B}_P} P_P^{(n)} g_{k,P}^{(n)} + N_0 \Delta_n}, \quad (1)$$

where $P_M^{(n)}$ and $P_P^{(n)}$ are the downlink transmit powers of macrocell M and picocell P on subcarrier n, respectively. The channel gain between user k and MBS M on subcarrier n is represented as $g_{k,M}^{(n)}$. The same gain between user k and Pico-BS P is $g_{k,P}^{(n)}$. The sets of MBSs and Pico-BSs in the simulation area are denoted by $\mathcal{B}_M$ and $\mathcal{B}_P$, respectively. The bandwidth of a subcarrier n is represented by Δ_n. The thermal noise power per Hz is N_0. The downlink transmission power of MBS M for cell-center MUEs that are in sector 1 can be calculated by

$$P_M = \frac{\beta_M P_{\max,M}}{N_A + \varepsilon_M N_B}, \quad (2)$$

where $P_{max,M}$ is the maximum transmission power of the MBS M. The downlink transmission power for cell-edge users is $\varepsilon_M P_M$. The downlink transmission power of the MBSs in other sectors can be obtained by replacing N_A and N_B with the corresponding number of subcarriers. We can use a similar approach to generate the SINR of picocell associated users (PUEs).

Consider sector s for which the sets of MUEs and PUEs are denoted by $\mathcal{K}_{M,s}$ and $\mathcal{K}_{P,s}$, respectively. We use k and n to denote the indices for users and subcarriers, respectively. We define vectors $\boldsymbol{C}_{M,s}$ and $\boldsymbol{C}_{P,s}$ to identify the regions of the MUEs and PUEs, respectively. When a user is classified in the cell-center region, then corresponding index of the vector will be 1, otherwise it will be 0. The matrices $\boldsymbol{F}_{M,s}$ and $\boldsymbol{F}_{P,s}$ indicate whether the subcarrier is assigned to MUEs and PUEs, respectively. If the subcarrier n is assigned to user k, the (n,k)th element of the matrix will be 1, otherwise it will be 0. The (n,k)th element of matrices $\boldsymbol{R}_1$ and $\boldsymbol{R}_2$ denote the throughput of MUE k on subcarrier n when the user is classified in the cell-center region and cell-edge region, respectively. The (n,k)th element of matrices $\boldsymbol{R}_3$ and $\boldsymbol{R}_4$ consist of the throughput of PUE k on subcarrier n when the user is classified in the cell-center and cell-edge region, respectively. Then, the total throughput of MUE k can be calculated as

$$R^{(M,k)} = \boldsymbol{C}_{M,s}^k \boldsymbol{F}_{M,s}^{(k,:)} \boldsymbol{R}_1^{(:,k)} + (1 - \boldsymbol{C}_{M,s}^k) \boldsymbol{F}_{M,s}^{(k,:)} \boldsymbol{R}_2^{(:,k)}. \quad (3)$$

We can use the same approach to calculate the throughput of PUEs and it can be written as

$$R^{(P,k)} = \boldsymbol{C}_{P,s}^k \boldsymbol{F}_{P,s}^{(k,:)} \boldsymbol{R}_3^{(:,k)} + (1 - \boldsymbol{C}_{P,s}^k) \boldsymbol{F}_{P,s}^{(k,:)} \boldsymbol{R}_4^{(:,k)}. \quad (4)$$

Note that $\boldsymbol{X}^{(n,:)}$ and $\boldsymbol{X}^{(:,k)}$ are the nth row vector of the matrix $\boldsymbol{X}$ and the kth column vector of the matrix $\boldsymbol{X}$, respectively. The throughput terms in (3) and (4) can be expanded by using the definitions in (1) as

$$\boldsymbol{R}_i^{(n,k)} = \Delta_n \log_2 \left(1 + \gamma_k^{(n)}\right), \quad \text{for all } i \in 1,2,3,4, \quad (5)$$

where $\boldsymbol{X}^{(n,k)}$ is the entry on the nth row and kth column of the matrix $\boldsymbol{X}$. Then, the aggregate throughput of sector s can

be calculated as

$$R_s = \sum_{k \in \mathcal{K}_{M,s}} R^{(M,k)} + \sum_{k \in \mathcal{K}_{P,s}} R^{(P,k)}. \tag{6}$$

A. Base Station Power Consumption Models

Modeling the energy consumption of the base stations has attracted some attention in the literature, see, e.g., [16]–[18]. In order to quantify the energy savings properly, we need a load-dependent model. In this paper, we use the power consumption model that is described in [16]. In this model, the power consumption of the base station is broken down into load-dependent and static power consumption parts. The load-dependent part depends on the transmission power of the base station. On the other hand, static power is constant and it will be consumed if the base station is on. If the base station has no user to serve, then it goes into the sleep mode. This model is given by

$$P_{Total} = \begin{cases} N_{TRX}\,(P_0 + \Delta \cdot P_{TX}) & 0 < P_{TX} \leq P_{\max} \\ N_{TRX} P_{sleep} & P_{out} = 0 \end{cases} \tag{7}$$

where P_{Total}, P_{TX}, and P_{sleep} are the overall power consumption of the base station, load-dependent transmission power, and the power consumption during the sleep mode. The maximum transmission power of the base station is denoted by $P_{\max}$. The number of the transceiver chains is represented by N_{TRX}. The slope of the load-dependent power consumption is Δ. By using this model, we can identify the power consumption of the MBSs and Pico-BSs. The overall power consumption of MBS M and Pico-BS P is denoted by P_M and P_P, respectively. The selection of these parameters are provided in Section V.

B. SE and EE Definition

Let $\nu_s(\boldsymbol{\varepsilon}, \boldsymbol{\beta})$ and $\eta_s(\boldsymbol{\varepsilon}, \boldsymbol{\beta})$ denote the SE and EE of sector s, respectively. They can be expressed as

$$\nu_s(\boldsymbol{\varepsilon}, \boldsymbol{\beta}) = \frac{R_s}{W_s} \text{ and } \eta_s(\boldsymbol{\varepsilon}, \boldsymbol{\beta}) = \frac{R_s}{\psi_s(\varepsilon_M, \boldsymbol{\beta}_s)}, \tag{8}$$

where the vectors $\boldsymbol{\varepsilon}$ and $\boldsymbol{\beta}$ denote the optimization variables of transmission power for all sectors in the network. The scalar parameter ε_M is the ε value of the MBS M in sector s. The vector $\boldsymbol{\beta}_s$ consists of all β values of the base stations in sector s. The total bandwidth allocated by MBS and Pico-BSs in sector s is denoted by W_s. The total power consumption in sector s is denoted by $\psi_s(\varepsilon_s, \boldsymbol{\beta}_s)$ which can be calculated as

$$\psi_s(\varepsilon_M, \boldsymbol{\beta}_s) = P_M + \sum_{P \in \mathcal{N}_{\text{Pico},s}} P_P, \tag{9}$$

where $\mathcal{N}_{\text{Pico},s}$ is the set of Pico-BSs in sector s.

III. Problem Formulation

In this section, we develop a framework to investigate the EE-SE tradeoff in multi-cell HetNets. Our objective is to maximize both EE and SE of the network while satisfying the rate requirements of users. As stated earlier, the problems of maximizing EE and SE usually do not coincide. Therefore, we introduce a multi-objective optimization-based formulation. The weighted summation method has been used to combine the EE and SE metrics. To ensure the units of these metrics are the same in weighted summation form, we multiply the SE function with W_{tot}/P_s. The parameter W_{tot} is the total bandwidth of the network and P_s is the total power consumption of sector s when all base stations transmit at the full power. A similar approach is also used in [15]. In addition, a unitless parameter α is introduced to tune the objective metric. This parameter is selected between 0 and 1 and when it increases the objective metric moves towards SE. It allows a service provider to make a judicious decision between two efficiency measures depending on their own criteria. During the peak hours, increasing SE is more important than the EE to satisfy the demand of the network. On the other hand, during the off-peak hours, maximizing EE becomes more important to save energy. A multi-objective optimization problem employing the variables we specified above can be defined as follows

$$\max_{\boldsymbol{\beta},\boldsymbol{\varepsilon},\mathbf{C},\mathbf{F}} \quad \sum_{s \in \mathcal{S}} (1-\alpha)\eta_s(\boldsymbol{\varepsilon}, \boldsymbol{\beta}) + \alpha \frac{W_{tot}}{P_s} \nu_s(\boldsymbol{\varepsilon}, \boldsymbol{\beta})$$

$$\text{s.t.} \quad R^{(M,k)} \geq R_{\min,k}, \text{for all } k \in \mathcal{K}_{M,s}, s \in \mathcal{S} \tag{10a}$$

$$R^{(P,k)} \geq R_{\min,k}, \text{for all } k \in \mathcal{K}_{P,s}, s \in \mathcal{S} \tag{10b}$$

$$\sum_{\substack{k \in \mathcal{K}_{M,s} \\ \boldsymbol{C}^k_{M,s}=1}} \boldsymbol{F}^{(k,n)}_{M,s} \leq 1 \text{ and } \sum_{\substack{k \in \mathcal{K}_{M,s} \\ \boldsymbol{C}^k_{M,s}=0}} \boldsymbol{F}^{(k,n)}_{M,s} = 0 \tag{10c}$$

for all $n \in \mathcal{N}^C_{M,s}, s \in \mathcal{S}$

$$\sum_{\substack{k \in \mathcal{K}_{M,s} \\ \boldsymbol{C}^k_{M,s}=0}} \boldsymbol{F}^{(k,n)}_{M,s} \leq 1 \text{ and } \sum_{\substack{k \in \mathcal{K}_{M,s} \\ \boldsymbol{C}^k_{M,s}=1}} \boldsymbol{F}^{(k,n)}_{M,s} = 0 \tag{10d}$$

for all $n \in \mathcal{N}^E_{M,s}, s \in \mathcal{S}$

$$\sum_{k \in \mathcal{K}_{M,s}} \boldsymbol{F}^{(k,n)}_{M,s} = 0 \quad \text{for all } n \notin \mathcal{N}^C_{M,s} \cup \mathcal{N}^E_{M,s}, s \in \mathcal{S} \tag{10e}$$

$$\sum_{\substack{k \in \mathcal{K}^p_{P,s} \\ \boldsymbol{C}^k_{P,s}=1}} \boldsymbol{F}^{(k,n)}_{P,s} \leq 1 \text{ and } \sum_{\substack{k \in \mathcal{K}^p_{P,s} \\ \boldsymbol{C}^k_{P,s}=0}} \boldsymbol{F}^{(k,n)}_{P,s} = 0 \tag{10f}$$

for all $n \in \mathcal{N}^C_{P,s}, p \in \mathcal{N}_{Pico,s}, s \in \mathcal{S}$

$$\sum_{\substack{k \in \mathcal{K}^p_{P,s} \\ \boldsymbol{C}^k_{P,s}=0}} \boldsymbol{F}^{(k,n)}_{P,s} \leq 1 \sum_{\substack{k \in \mathcal{K}^p_{P,s} \\ \boldsymbol{C}^k_{P,s}=1}} \boldsymbol{F}^{(k,n)}_{P,s} = 0 \tag{10g}$$

for all $n \in \mathcal{N}^E_{P,s}, p \in \mathcal{N}_{Pico,s}, s \in \mathcal{S}$

$$\sum_{k \in \mathcal{K}^p_{P,s}} \boldsymbol{F}^{(k,n)}_{P,s} = 0 \quad \text{for all } n \notin \mathcal{N}^C_{P,s} \cup \mathcal{N}^E_{P,s},$$

$$p \in \mathcal{N}_{Pico,s}, s \in \mathcal{S} \tag{10h}$$

$$\boldsymbol{\varepsilon} \succeq \mathbf{0} \text{ and } \mathbf{0} \preceq \boldsymbol{\beta} \preceq \mathbf{1}, \tag{10i}$$

where $\mathcal{S}$ is the set of all sectors in the simulation area. The rate requirement of user k is denoted by $R_{\min,k}$. The parameters $\mathcal{N}^C_{M,s}$ and $\mathcal{N}^E_{M,s}$ are the set of subcarriers that are assigned to cell-center and cell-edge MUEs, respectively. Likewise, the parameters $\mathcal{N}^C_{P,s}$ and $\mathcal{N}^E_{P,s}$ are the set of subcarriers that are assigned to cell-center and cell-edge PUEs, respectively. The set of PUEs that are associated with Pico-BS P is denoted by $\mathcal{K}^P_{P,s}$. The notation $\mathbf{x} \succeq \mathbf{0}$ forces that each element of vector $\mathbf{x}$ is greater than or equal to 0. Constraints (10a) and (10b) ensure that rate constraints of the users are satisfied. Constraints (10c) to (10h) guarantee that available resources to a base station

for a region are assigned to users that are associated with the base station and in the corresponding region and unavailable resources are not assigned to these users. Constraint (10i) guarantees that parameters $\boldsymbol{\varepsilon}$ and $\boldsymbol{\beta}$ are within the given limits.

The objective function in (10) is non-convex, therefore the optimal solution requires exhaustive search over all possible cell-center radii, frequency assignments, and power levels for all sectors. To tackle this problem, we divide our problem into $|S|$ subproblems so that each sector maximizes its own objective function. This resource allocation problem still needs to be solved over the cell-center radius, frequency, and power domains jointly. This problem is combinatorial over the first two domains and non-convex over the power allocation domain [19], [20]. Therefore, obtaining the optimum solution requires exhaustive search over all domains. For that reason, instead of solving these problems jointly, we propose a three-stage algorithm that solves each problem consecutively. In the next section, we will describe these stages and discuss the convergence analysis of the proposed algorithm.

IV. Proposed Solution

Our formulation in (10) enables us to develop an energy- and spectral-efficient resource allocation algorithm. Our proposed algorithm decouples the problem into three stages and solves them iteratively. First, we select the cell-center radius to divide the sector area into cell-center and cell-edge regions. Second, MBS and Pico-BSs assign frequency resources to their users. Last, we determine the power control parameters ε and $\boldsymbol{\beta}$ in each sector. The rate requirements of the users are included in the power control subproblem by using dual decomposition techniques. After these three stages, each MBS sends the updated information to the other base stations in the network. Then, these stages are repeated again with the updated information until convergence. The proposed algorithm is presented under the heading Algorithm 1. In the sequel, we discuss each stage of the proposed algorithm in detail.

A. The Cell-Center Region Boundaries

In the first stage of the proposed algorithm, we need to set the cell-center region boundaries in each sector to select the region of the MUEs and also determine the available resources to Pico-BSs. In our prior work [6], we proposed two cell-center radius selection algorithms and demostrated that more than two times gain can be obtained in terms of EE and throughput by proper selection of cell-center radii. However, neither of these algorithms considers the rate requirements of users. Therefore, a dynamic algorithm is proposed in this paper. The optimum cell-center radius that maximizes the objective function requires exhaustive search over all possible radii. In addition, the frequency assignment problem that will be discussed in the next subsection needs to be solved again for each radius selection. Therefore, we propose an iterative algorithm in this paper. The proposed algorithm compares the Lagrangian function of the current cell-center radius with two cell-center radii: one more MUE or Pico-BS is included in the cell-center region from the cell-edge region and one more MUE or Pico-BS is excluded to the cell-edge region from the cell-center region. Among these three cell-center radii, the one that maximizes the Lagrangian function is selected as the cell-center radius. This process is repeated until the optimal cell-center radius is determined.

Algorithm 1 Proposed Energy- and Spectral-Efficient Resource Allocation Algorithm

1: **Initialize:** $r_{th,s}^{(0,c)} = r_{r,s}/2 \quad (\varepsilon_s^{(0)}, \beta_s^0, \boldsymbol{\beta}_{P,s}^{(0)}) = [1, 1, \mathbf{1}]$
2: $r_{th,s}^{(t,c)} = r_{th,s}^{(t-1,c)}$
3: **Stage 1:** Three-candidate cell-center region boundaries are selected by using the cell-center radius algorithm in Section IV-A: $r_{th,s}^{(t,c-1)}$, $r_{th,s}^{(t,c)}$, and $r_{th,s}^{(t,c+1)}$.
4: **for** $n := -1$ to 1 **do**
5: **Stage 2:** For $r_{th,s}^{(t,c+n)}$, frequency assignment problem is solved by using the algorithm in Section IV-B for each base station in the sector.
6: the Lagrangian functions $\mathcal{L}_s^{(n)}$, which is described in the Section IV-C, is calculated.
7: **end for**
8: Among all three Lagrangian function, the maximum one is selected for the cell-center region boundary and the frequency assignments.
9: **Stage3:** Then, the power control algorithm, which is described in Section IV-C, determines the optimal power control parameters.
10: Go to Step 2 and repeat until the convergence.

B. Frequency Assignment Problem

In the second stage of the algorithm, frequency resources are assigned to the users. In the literature, several scheduling algorithms are discussed, see, e.g., [21]. Each scheduler has its own priorities such as minimizing latency, maximizing fairness, etc. In this paper, we propose an opportunistic (OPP) scheduler algorithm. The proposed algorithm shares resources fairly among users, decreases outage probabilities, increases SE, and satisfies the rate requirements of users. Due to the fact that the smallest granularity is the resource block in the LTE systems, the proposed algorithm assigns resources in this level.

OPP Scheduler: The OPP scheduler shares resource blocks among users to satisfy the rate requirements of users and to maximize the objective metric. Due to the fact that the cell-center and cell-edge MUEs are allocated different subbands, this algorithm runs for both sets separately in MBSs. The proposed algorithm first assigns one resource block to each user due to the fairness. Each user is assigned the resource block that has the best average channel gain among the available resource blocks. If there are more resource blocks than users, remaining resource blocks are assigned to the users by the following rule. First, users that could not satisfy their rate requirements are sorted in descending order according to the difference between their rate requirements and their actual rates. Second, the resource block that has the best average channel gain among the available resource blocks is assigned to the user with the largest difference. Then, users are sorted again with the updated rates. This process continues until all available resource blocks are assigned or the rate requirements of all users are satisfied. If there are still unassigned resource blocks, these resources are assigned to the user with the best

average channel gain to increase the SE of then network. This process continues until all the resource blocks are assigned.

C. Power Control Problem

In the third stage of the algorithm, we determine the power levels on each subband that maximize our objective and also satisfy the rate requirements of the users. Given the cell-center radius vector and frequency assignment matrix, we need to determine the power control parameters $\boldsymbol{\beta}_s$ and ε_s. We use convex optimization techniques to obtain optimum $\boldsymbol{\beta}_s$ and ε_s parameters.

Lemma 1. *The energy and spectral efficiency per sector expression* $(1-\alpha)\eta_s(\boldsymbol{\varepsilon},\boldsymbol{\beta}) + \alpha\frac{W_{tot}}{P_s}\nu_s(\boldsymbol{\varepsilon},\boldsymbol{\beta})$ *in (10) is quasiconcave in* ε_s *and* $\boldsymbol{\beta}_s$.

Proof : The Proof is given in the online Appendix [22].

While obtaining optimum power control parameters, we assume that the power control parameters of the other sectors are constant. Therefore, the interference conditions from the other sectors are assumed to be constant. However, if base stations increase their transmission powers to high levels without considering the other sector, this harms the transmissions in other sectors and causes outages and decrease in the overall utility. To prevent this, we implement the interference-based pricing mechanism that penalizes each base station by the amount of the interference it creates. This approach was first proposed in [7]–[9]. We use $\theta_s(\varepsilon_s,\boldsymbol{\beta}_s)$ to denote the interference pricing function for sector s. The penalty function increases with the interference that the base station creates and becomes more severe if the interference causes outages of users in other sectors.

Section IV-B guarantees that constraints (10c) to (10h) is satisfied for each base station. Then, we can write the Lagrangian of the problem (10) for the remaining constraints as follows

$$\begin{aligned}\mathcal{L}_s(\mathbf{x}_s) &= (1-\alpha)\eta_s(\boldsymbol{\varepsilon},\boldsymbol{\beta}) + \alpha\frac{W_{tot}}{P_s}\nu_s(\boldsymbol{\varepsilon},\boldsymbol{\beta}) - \theta_s(\varepsilon_s,\boldsymbol{\beta_s}) \\ &- \sum_{k\in\mathcal{K}_{M,s}}\lambda_{k,s}(R_{\min,k}-R^{(M,k)}) - \sum_{k\in\mathcal{K}_{P,s}}\lambda_{k,s}(R_{\min,k}-R^{(P,k)}) \\ &+\tau_M^L\beta_M + \tau_M^U(1-\beta_M) + \sum_{P\in\mathcal{N}_{\text{Pico},s}}\tau_P^L\beta_P + \\ &\sum_{P\in\mathcal{N}_{\text{Pico},s}}\tau_P^U(1-\beta_P) + \rho_s\varepsilon_M.\end{aligned} \tag{11}$$

For simplicity, we will use $\mathcal{L}_s$ for $\mathcal{L}(\varepsilon_s,\boldsymbol{\beta}_s,\boldsymbol{\lambda},\boldsymbol{\tau_s^L},\boldsymbol{\tau_s^U},\rho_s)$ throughout the rest of the paper.

In this paper, the transmission power of the MBS M depends on β_M and ε_M and the transmission power of the Pico-BS P depends on β_P. The interference pricing function accounts for the interference that all base stations in the sector s are subject to. We define a vector, $\mathbf{z}_s = [\beta_M \;\; \varepsilon_M \;\; \beta_P^1 \ldots \beta_P^{N_{P,s}}]$ where $N_{P,s}$ is the number of Pico-BSs in sector s. Then, we can write the interference pricing function as follows

$$\theta_s(\varepsilon_s,\boldsymbol{\beta}_s) = \mathbf{z}_s^T\sum_{\substack{s'\in\mathcal{S}\\ s'\neq s}}\nabla_{\mathbf{z}_s}\mathcal{L}_{s'}. \tag{12}$$

The pricing function reflects the marginal costs of the variables β_M, ε_M, and β_Ps for all Pico-BSs.

In each sector, there are $2+N_{Picos}$ power control parameters. In order to obtain the optimum power control parameters, we will employ the Levenberg-Marquardt method. The Levenberg-Marquardt method is a variant of the Newton method and provides quadratic convergence. The quadratic approximation of the Lagrangian function in (11) can be expressed as

$$g(\mathbf{z}) = \mathcal{L}_s + \nabla\mathcal{L}_s^T(\mathbf{z}-\mathbf{z}_s^{(t,l)}) + \frac{1}{2}(\mathbf{z}-\mathbf{z}_s^{(t,l)})^T\nabla^2\mathcal{L}_s(\mathbf{z}-\mathbf{z}_s^{(t,l)}), \tag{13}$$

where l and t denote the Newton iteration and time instant, respectively. The Hessian matrix of the $\mathcal{L}_s$ at $\mathbf{z}_s^{(t,l)}$ is denoted by $\nabla^2\mathcal{L}_s$. Then, the power control parameters that maximize $g(\mathbf{z})$ can be obtained by

$$\mathbf{z}_s^{(t,l+1)} = \mathbf{z}_s^{(t,l)} - \mu_l(\nabla^2\mathcal{L}_s^{(l)} - \xi\mathbf{I})^{-1}\nabla\mathcal{L}_s^{(l)}, \tag{14}$$

where $\mathbf{I}$ is the identity matrix. The term $\xi\mathbf{I}$ should be selected in such a way that all the eigenvalues of $\mathbf{D} = (\nabla^2\mathcal{L}_s^{(l)} - \xi\mathbf{I})$ are negative. This approach guarantees that $\mathbf{D}$ is negative definite. The parameter ξ should be selected larger than the highest positive eigenvalue of the $\nabla^2\mathcal{L}_s^{(l)}$. If all eigenvalues of $\nabla^2\mathcal{L}_s^{(l)}$ are already negative, then ξ should be selected as 0 and the Levenberg-Marquardt works as the Netwon method. The proposed algorithm is depicted under the heading Algorithm 2. The parameter $l_{\max}$ is the maximum number of iterations, and ϵ is a control parameter to determine when to exit the algorithm when the changes between two iterations is sufficiently small. We use a controlled increase mechanism for the power control updates. If the difference between the power control parameters during two consecutive time instants is large, it may cause the interference pricing mechanism not to accurately estimate the prices [8]. Therefore, the controlled increase mechanism is employed in this paper. The controlled increase mechanism in Step 16 prevents the base stations from changing their transmission powers by a large amount. The parameter ζ is selected as $t/(2t+1)$ [23].

1) Complexity Anlaysis

The main computational effort of the proposed algorithm is calculating the eigenvalues of the matrix $\mathbf{D} = (\nabla^2\mathcal{L}_s^{(l)} - \xi\mathbf{I})$ and taking the inverse of the same matrix. Therefore, the complexity of the proposed power control increases with the number of power control parameters. When the number of Pico-BSs in the sector increases, the complexity of the algorithm increases with N_{Picos}^3. For example, when there are 2 Pico-BSs in each sector, the matrix becomes 4×4 and taking the inverse of this matrix is straightforward with today's processing capacities.

V. Numerical Results

In this section, we evaluate the performance of the proposed algorithm. We investigate the effect of the parameter α over the EE-SE tradeoff and outage probabilities.

First, we will describe our simulation environment. In the FFR method, we first assign 14 resource blocks to subband A, and then the remaining 36 are evenly distributed among the subbandds B, C, and D. In our simulation area, 19 MBSs are

Algorithm 2 Proposed Power Control Algorithm with Pricing

1: **Initialize:** $\mathbf{z}_s^{(t,0)} = (\varepsilon_M^{(t-1,l_{max}+1)} \ \boldsymbol{\beta}_s^{(t-1,l_{max}+1)^T})$ and set $l = 0$
2: % Each sector solves (11) by using the Levenberg-Marquardt Method
3: **for** $l := 1$ to $l_{\max}$ **do**
4: **if** $\omega_{\max} = \max(\text{eig}(\nabla^2_{\mathbf{z}} \mathcal{L}_s^{(l)})) < 0$ **then**
5: $\xi = 0$.
6: **else**
7: $\xi = \omega_{\max} + \sigma$.
8: **end if**
9: $\mathbf{d}_l^{LM} = -(\nabla^2 \mathcal{L}_s^{(l)} - \xi \mathbf{I})^{-1} \nabla \mathcal{L}_s^{(l)}$.
10: Update the power control parameters, $\mathbf{z}_s^{(l+1)}$, using

$$\mathbf{z}_s^{(t,l+1)} = \mathbf{z}_s^{(t,l)} + \mu_l \mathbf{d}_l^{LM},$$

11: Update the Lagrange multiplier, $\lambda_{k,s}^{(l+1)}$ for all $k \in \mathcal{K}_{M,s}$ and $j \in \mathcal{K}_{P,s}$, using

$$\lambda_{k,s}^{(l+1)} = \left[\lambda_{k,s}^{(l)} + \phi_{k,s}(R_{\min,k} - R^{(M,k)})\right]^+, \text{and}$$

$$\lambda_{j,s}^{(l+1)} = \left[\lambda_{j,s}^{(l)} + \phi_{j,s}(R_{\min,j} - R^{(P,j)})\right]^+.$$

12: **if** $\left|\nabla \mathcal{L}_s^T \mathbf{d}_l^{LM}\right| \leq \epsilon$ **then**
13: **Break**
14: **end if**
15: **end for**
16: $\mathbf{z}_s^{(t,l_{max}+1)} = (1-\zeta)\mathbf{z}_s^{(t-1,l_{max}+1)} + \zeta \mathbf{z}_s^{(t,l_{max})}$
17: *Price Update:* Each user calculates interference prices and feds these values back to its base station.
18: Go to Step 2 and repeat.

deployed and each of them employs 3-sector antennas. We use the wraparound technique to avoid edge effects. Two Pico-BSs are randomly deployed in each sector area. In each sector, we generate 20 users. First, we generate two users within a 40 meter radius of the Pico-BSs. Then, the rest of the users are randomly generated under the settings in Table II. The highest RSRP method is used for the cell associations. Even though we generate two users close to Pico-BSs, they are not forced to associate with the Pico-BSs. The rest of the simulation parameters are given in Table II [24].

Figs. 2(a)-(b) illustrate the average EE and SE of the sectors for different α values for three cases: no-rate constraint and rate constraints of 128 kbps and 512 kbps. As expected, the average EE of the network decreases with α for all three cases. When there are no rate constraints and α is equal to 0, the average EE of the network reaches its highest point and it becomes 452.81 kbits/Joule. When we increase α for the no-rate-constraint case, the average EE decreases and becomes 437.45, 423.20, 390.71, and 366.18 kbits/Joule when α is $0.25, 0.5, 0.75$, and 1, respectively. Sacrificing 2.4% SE gain can be transformed to 23.4% EE gain. The SE increases with α, however the changes are not as dramatic as the EE. The average SE of the network increases 2.4% when we increase α from 0 to 1, when users do not have any rate requirements. When users have rate requirements, both EE and SE of the network decreases. When α is equal to 0,

Table II
SIMULATION PARAMETERS

Parameter	Setting
Channel bandwidth	10 MHz
Total number of RBs	50 RBs
Freq. selective channel model (CM)	Extended Typical Urban CM
UE to MBS PL model	$128.1 + 37.6 \log_{10}(d)$
UE to Pico-BS PL model	$140.7 + 36.7 \log_{10}(d)$
Effective thermal noise power, N_0	-174 dBm/Hz
UE noise figures	9 dB
MBS and Pico-BS antenna gain	14 dBi and 5 dBi
UE antenna gain	0 dBi
Antenna horizontal pattern, $A(\theta)$	$-\min(12(\theta/\theta_{3\text{dB}})^2, A_m)$
A_m and $\theta_{3\text{dB}}$	20 dB and 70°
Penetration loss	20 dB
Macrocell and picocell shadowing	8 dB and 10 dB
Inter-site distance	500 m
Minimum MBS to user distance	50 m
Minimum Pico-BS to user distance	10 m
Minimum Pico-BS to MBS distance	75 m
Minimum Pico-BS to Pico-BS distance	40 m
Traffic model	Full buffer
Power Consumption Parameters	MBS: (130W, 75W, 46dBm, 4.7)
(P_0, P_{sleep}, $P_{\max}$, Δ)	Pico-eNB: (56W, 39W, 30dBm, 2.6)

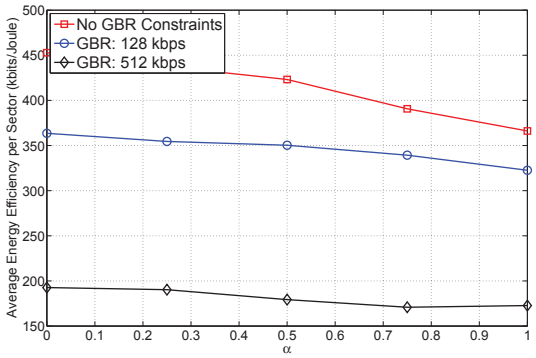

(a)

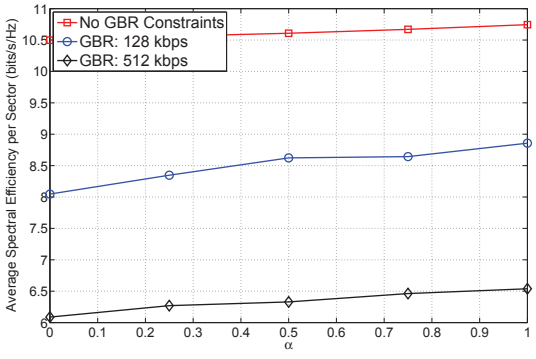

(b)

Figure 2. The average EE per sector (a) and average SE per sector (b) for different α values.

EE of the networks drops 20% and 57% and the SE of the network drops 23% and 42.2% for the rate constraints 128 kbps and 512 kbps compared to the no-rate constraint case, respectively. In order to satisfy the rate constraints of the users, base stations increase their transmission powers. This causes increase in the intercell interference and decrease in the SE. In addition, when we increase the rate constraints, some MUEs cannot satisfy their rate requirements. Therefore, Pico-BSs that create interference to these users decrease their

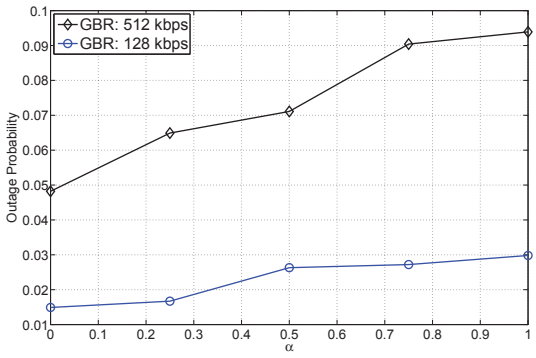

Figure 3. The outage probabilities of users for different α values when rate requirements of users are 128 kbps and 512 kbps.

transmission powers. This leads to decrease in the SE of the network. Note from Fig. 2 that in all three cases, improving EE decreases SE and vice versa. Therefore, all points of the vector $(\eta_s(\boldsymbol{\varepsilon},\boldsymbol{\beta}), \nu_s(\boldsymbol{\varepsilon},\boldsymbol{\beta}))$ are Pareto optimal for $0 \leq \alpha \leq 1$.

Second, we investigate the relation between the parameter α and outage probabilities. In Fig. 3, we investigate two cases, when the rate requirements of users are 128 kbps and 512 kbps. The outage probability is not defined when users do not have a rate requirement. It can be observed that when we increase the parameter α, the outage probabilities increase. When α is equal to 0, the outage probabilities are 1.49% and 4.82% corresponding to the rate requirements 128 kbps and 512 kbps, respectively. The outage probabilities increase with the parameter α and become 2.98% and 9.39% for $\alpha = 1$ when rate requirements are 128 and 512 kbps, respectively. When α increases, in order to increase the SE of the network, base stations increase their transmission powers. Therefore, users with worse channel conditions suffer from the increased interference and the number of users that are in outage increases.

VI. Conclusion

In this paper, we studied the EE-SE tradeoffs in multi-cell heterogeneous wireless networks. We defined the problem as multi-objective optimization and proposed a three-stage algorithm that solves cell-center boundary selection problem, frequency assignment problem, and power control problem separately.In each stage of the proposed algorithm, the rate requirements of users are taken into account. A dynamic cell-center boundary selection algorithm determines the regions of MUEs and Pico-BSs and available resources to these base stations. In addition, the opportunistic scheduling mechanism distributes the resources in order to satisfy the rate requirements of users and also to increase the objective metric of the network. Furthermore, we employ a Levenberg-Marquardt method-based power allocation algorithm to solve the power control problem. Based on our results, first the tradeoff between EE and SE can be adjusted via the weight of the multi-objective function. Second, we can obtain 23.4% improvement in terms of EE by sacrificing 2.4% SE. Third, increasing SE of the network leads higher outage probabilities due to the increased intercell-interference.

References

[1] K. Davaslioglu and E. Ayanoglu, "Quantifying potential energy efficiency gain in green cellular wireless networks," *IEEE Communications Surveys and Tutorials*, vol. 16, no. 4, pp. 2065–2091, Fourth Quarter 2014.

[2] A. Ghosh, N. Mangalvedhe, R. Ratasuk, B. Mondal, M. Cudak, E. Visotsky, T. Thomas, J. Andrews, P. Xia, H. Jo, H. Dhillon, and T. Novlan, "Heterogeneous cellular networks: From theory to practice," *IEEE Commun. Mag.*, vol. 50, no. 6, pp. 54–64, Jun. 2012.

[3] G. Boudreau, J. Panicker, N. Guo, R. Chang, N. Wang, and S. Vrzic, "Interference coordination and cancellation for 4G networks," *IEEE Commun. Magazine*, vol. 47, no. 4, pp. 74–81, April 2009.

[4] H. Holma and A. Toskala, *LTE-Advanced: 3GPP Solution for IMT-Advanced*. West Sussex, U.K.: John Wiley & Sons, Ltd, 2012.

[5] N. Saquib, E. Hossain, and D. I. Kim, "Fractional frequency reuse for interference management in LTE-Advanced HetNets," *IEEE Wireless Commun.*, vol. 20, no. 2, pp. 113–122, Apr. 2013.

[6] K. Davaslioglu, C. Coskun, and E. Ayanoglu, "Energy-efficient resource allocation for fractional frequency reuse in heterogeneous networks," *IEEE Trans. Wireless Commun.*, vol. 14, no. 10, pp. 5484–5497, Oct 2015.

[7] J. Huang, R. Berry, and M. Honig, "Distributed interference compensation for wireless networks," *IEEE J. Sel. Areas Commun.*, vol. 24, no. 5, pp. 1074–1084, May 2006.

[8] C. Shi, R. Berry, and M. Honig, "Distributed interference pricing for OFDM wireless networks with non-separable utilities," in *Proc. Annu. Conf. Inform. Sciences and Systems (CISS)*, Mar. 2008, pp. 755–760.

[9] ——, "Monotonic convergence of distributed interference pricing in wireless networks," in *Proc. IEEE Int. Symp. Information Theory (ISIT)*, June 2009, pp. 1619–1623.

[10] C. Xiong, G. Li, S. Zhang, Y. Chen, and S. Xu, "Energy- and spectral-efficiency tradeoff in downlink OFDMA networks," *IEEE Trans. Wireless Commun.*, vol. 10, no. 11, pp. 3874–3886, November 2011.

[11] Y. Li, M. Sheng, C. Yang, and X. Wang, "Energy efficiency and spectral efficiency tradeoff in interference-limited wireless networks," *IEEE Commun. Letters*, vol. 17, no. 10, pp. 1924–1927, October 2013.

[12] D. Tsilimantos, J. Gorce, and K. Jaffrès-Runser, "Spectral and energy efficiency trade-off with joint power-bandwidth allocation in OFDMA networks," *CoRR*, vol. abs/1311.7302, 2013.

[13] R. Marler and J. Arora, "Survey of multi-objective optimization methods for engineering," *Structural and Multidisciplinary Optimization*, vol. 26, no. 6, pp. 369–395, 2004.

[14] C. He, B. Sheng, P. Zhu, X. You, and G. Li, "Energy- and spectral-efficiency tradeoff for distributed antenna systems with proportional fairness," *IEEE Journal on Selected Areas in Commun.*, vol. 31, no. 5, pp. 894–902, May 2013.

[15] J. Tang, D. So, E. Alsusa, and K. Hamdi, "Resource efficiency: A new paradigm on energy efficiency and spectral efficiency tradeoff," *IEEE Trans. Wireless Commun.*, vol. 13, no. 8, pp. 4656–4669, Aug 2014.

[16] G. Auer *et al.*, "How much energy is needed to run a wireless network?" *IEEE Wireless Commun.*, vol. 18, no. 5, pp. 40–49, Oct. 2011.

[17] F. Richter, A. Fehske, and G. Fettweis, "Energy efficiency aspects of base station deployment strategies for cellular networks," in *Proc. IEEE Veh. Technol. Conf.*, Sep. 2009, pp. 1–5.

[18] H. Holtkamp, G. Auer, V. Giannini, and H. Haas, "A parameterized base station power model," *IEEE Commun. Letters*, vol. 17, no. 11, pp. 2033–2035, Nov. 2013.

[19] L. Hoo, B. Halder, J. Tellado, and J. Cioffi, "Multiuser transmit optimization for multicarrier broadcast channels: Asymptotic FDMA capacity region and algorithms," *IEEE Trans. Commun.*, vol. 52, no. 6, pp. 922–930, Jun. 2004.

[20] W. Yu, "Multiuser water-filling in the presence of crosstalk," in *Proc. Inform. Theory and Appl. (ITA) Workshop*, Jan 2007, pp. 414–420.

[21] S. Sesia, I. Toufik, and M. Baker, *LTE - The UMTS Long Term Evolution: From Theory to Practice*. West Sussex, U.K.: Wiley, 2009.

[22] C. C. Coskun and E. Ayanoglu, "Energy-spectral efficiency trade-off for heterogeneous networks with QoS constraints (Appendix)," October 2016. [Online]. Available: http://newport.eecs.uci.edu/ ayanoglu/EESE.pdf

[23] Z. Han, D. Niyato, W. Saad, T. Başar, and A. Hjørungnes, *Game Theory in Wireless and Communication Networks: Theory, Models, and Applications*. Cambridge, U.K.: Cambridge Univ. Press, 2012.

[24] 3GPP, TR 36.814, "Further advancements for E-UTRA physical layer aspects (Release 9)," Mar. 2010.